



HAL
open science

Hyperfine excitation of C2H and C2D by para-H2

Fabien Dumouchel, François Lique, Annie Spielfiedel, Nicole Feautrier

► **To cite this version:**

Fabien Dumouchel, François Lique, Annie Spielfiedel, Nicole Feautrier. Hyperfine excitation of C2H and C2D by para-H2. Monthly Notices of the Royal Astronomical Society, 2017, 471 (2), pp.1849 - 1855. 10.1093/mnras/stx1707 . hal-01919497

HAL Id: hal-01919497

<https://normandie-univ.hal.science/hal-01919497>

Submitted on 8 Dec 2023

HAL is a multi-disciplinary open access archive for the deposit and dissemination of scientific research documents, whether they are published or not. The documents may come from teaching and research institutions in France or abroad, or from public or private research centers.

L'archive ouverte pluridisciplinaire **HAL**, est destinée au dépôt et à la diffusion de documents scientifiques de niveau recherche, publiés ou non, émanant des établissements d'enseignement et de recherche français ou étrangers, des laboratoires publics ou privés.

Hyperfine excitation of C₂H and C₂D by *para*-H₂

Fabien Dumouchel,¹★ François Lique,^{1,2}★ Annie Spielfiedel²† and Nicole Feautrier²

¹LOMC-UMR 6294, CNRS-Université du Havre, 25 rue Philippe Lebon, BP 1123, F-76 063 Le Havre cedex, France

²LERMA, Observatoire de Paris, PSL Research University, CNRS, Sorbonne Université, UPMC University Paris 06, F-92195 Meudon, France

Accepted 2017 July 5. Received 2017 July 3; in original form 2017 June 7

ABSTRACT

The [C₂H]/[C₂D] abundance ratio is a useful tool to explore the physical and chemical conditions of cold molecular clouds. Hence, an accurate determination of both the C₂H and C₂D abundances is of fundamental interest. Due to the low density of the interstellar medium, the population of the energy levels of the molecules is not at local thermodynamical equilibrium. Thus, the accurate modelling of the emission spectra requires the calculation of collisional rate coefficients with the most abundant interstellar species. Hence, we provide rate coefficients for the hyperfine excitation of C₂H and C₂D by *para*-H₂(*j*=0), the most abundant collisional partner in cold molecular clouds. State-to-state rate coefficients between the lowest levels were computed for temperatures ranging from 5 to 80 K. For both isotopologues, the $\Delta j = \Delta F$ propensity rule is observed. The comparison between C₂H and C₂D rate coefficients shows that differences by up to a factor of two exist, mainly for $\Delta j = \Delta N = 1$ transitions. The new rate coefficients will significantly help in the interpretation of recent observed spectra.

Key words: molecular data – molecular processes – scattering.

1 INTRODUCTION

The C₂H ethynyl radical was first detected in the interstellar medium (ISM) by Tucker, Kutner & Thaddeus (1974). They observed four components of the $N = 1 \rightarrow 0$ rotational transition in several sources associated with massive star-forming regions. Then, its rotational spectrum was studied in the laboratory at different millimetre and submillimetre wavelengths (Sastry et al. 1981; Gottlieb, Gottlieb & Thaddeus 1983; Müller, Klaus & Winnewisser 2000; Brünken et al. 2007) in order to have accurate information on the fine structure splitting of the rotational states. Indeed, C₂H is a $^2\Sigma^+$ electronic ground state and the Hund's case (b) limit is well suited to describe the pattern of internal energy levels. Hence, the total angular momentum *j* of the molecule is formed as the vector sum of the rotational *N* and electronic spin *S* angular momenta, such as $\mathbf{j} = \mathbf{N} + \mathbf{S}$.

C₂H is found to be a very abundant interstellar molecule in standard galactic sources (e.g. Orion, TMC-1) as well as in other types of sources including photo dominated regions (PDRs) (Teyssier et al. 2004; Cuadrado et al. 2015), diffuse clouds (Lucas & Liszt 2000), protoplanetary discs (Dutrey, Guilloteau & Guelin 1997), pre-stellar cores (Padovani et al. 2009) and high-mass star-forming regions (Beuther et al. 2008). C₂H is by far the most abundant of the interstellar unsaturated hydrocarbons. Depending

on the environment, different rotational transitions can be observed. Recently, the lines associated with the $N = 1 \rightarrow 0$, $N = 2 \rightarrow 1$, $N = 3 \rightarrow 2$ and $N = 4 \rightarrow 3$ transitions were observed in the PDR Orion Bar, and the lines associated with transitions up to $N = 10 \rightarrow 9$ were detected in a hotter gas (Cuadrado et al. 2015).

C₂D (as well as ¹³CCH and C¹³CH) is also detected and first observed towards the Orion A ridge and Orion KL star-forming regions (Combes et al. 1985; Vrtilek et al. 1985; Saleck et al. 1994). Although the interstellar ratio of deuterium to hydrogen ([H]/[D]) is only $\approx 10^{-5}$ (Roberts & Millar 2000; Pety et al. 2005), the observed degree of deuterium fraction (i.e. the [C₂H]/[C₂D] abundance ratio) is enhanced by large factors in various astrophysical environments, including cold dense cores (Guelin, Langer & Wilson 1982), circumstellar discs (van Dishoeck, Thi & van Zadelhoff 2003; Guilloteau et al. 2006), hot molecular cores (Hatchell, Millar & Rodgers 1998) and PDRs (Leurini et al. 2006; Treviño-Morales et al. 2014). With abundances that strongly depend on the reaction pathways involved in their formation, deuterated species are important indicators of the physical and chemical evolution of molecular clouds. As an example, the abundance ratio [C₂D]/[C₂H] varies from 0.02 to 0.08 in the ultracompact HII region Mon R2, according to the observed position, so that [C₂D]/[C₂H] is found to be a possible ‘good chemical clock’ for the evolutionary stage of massive star-forming regions (Treviño-Morales et al. 2014).

In addition to their fine structure that can easily be resolved in astronomical spectra, the C₂H and C₂D species exhibit a hyperfine structure because H and D atoms possess a non-zero nuclear spin ($I = 0.5$ for H and $I = 1$ for D). Hence, the energy levels of C₂H and C₂D are characterized by the quantum numbers *j* and *F*, where

* E-mail: fabien.dumouchel@univ-lehavre.fr (FD); francois.lique@univ-lehavre.fr (FL)

† Deceased on 2016 December 14.

F results from the coupling of j with I ($\mathbf{F} = \mathbf{j} + \mathbf{I}$). Each hyperfine level is labelled by a quantum number F varying between $|I - j|$ and $I + j$.

Due to the low density of the interstellar medium, the energy levels of the molecules are not at local thermodynamical equilibrium. Thus, the modelling of molecular emission of these species requires excitation calculations using radiative as well as collisional rate coefficients with the most abundant interstellar species that are generally He and H_2 in the cold ISM.

Fine- and hyperfine-structure resolved rate coefficients were calculated for the collisional excitation of C_2H by He (Spielfiedel et al. 2013) for temperatures ranging from 5 to 100 K. Transitions involving the lowest 25 fine-structure levels of C_2H were considered. Recently, collisional excitation by *para*- H_2 ($j=0$) was also studied using a new *ab initio* potential energy surface (PES) and rate coefficients for (de-)excitation between the 25 lowest fine-structure levels of C_2H were computed for temperatures up to 100 K (Najar et al. 2014, hereafter Paper I). By comparing the He and H_2 rate coefficients for all fine-structure resolved transitions, it was found that the ratio between the rate coefficients varies from 1 to 10 depending on the transitions. In Paper I, the hyperfine structure of C_2H was neglected. However, hyperfine-resolved data are needed by the astrophysical community, especially for modelling cold molecular cloud emission spectra. In this work, we aim at determining the temperature variation of the hyperfine-resolved $\text{C}_2\text{H}-\text{H}_2$ rate coefficients. In addition, we also aim to provide the first $\text{C}_2\text{D}-\text{H}_2$ rate coefficients that would be very useful for analysing the $[\text{C}_2\text{D}]/[\text{C}_2\text{H}]$ abundance ratio. As we will see, the comparison between the C_2H and C_2D rate coefficients will point out the effects of the isotopic substitution in the magnitude of the collisional data and confirms that it is risky to use rate coefficients of the main isotopologue to analyse secondary isotopologue emission spectra as already noticed for NH/ND (Dumouchel et al. 2012), $\text{H}_2\text{O}/\text{HDO}$ (Faure et al. 2012) and $\text{NH}_3/\text{NH}_2\text{D}$ (Wiesenfeld, Scribano & Faure 2011).

This paper is organized as follows. Section 2 provides a brief description of the PES and describes some theoretical aspects of the scattering calculations. Collisional rate coefficients between hyperfine levels are presented in Section 3 for temperatures up to 80 K. A comparison between C_2H and C_2D results is also presented. Concluding remarks are drawn in Section 4.

2 COMPUTATIONAL METHODOLOGY

2.1 Potential energy surface

In the scattering calculations, we employed the PES described in detail in Paper I. Here, we just describe the main features of the PES.

The C_2H radical in its ground $X^2\Sigma^+$ electronic state has a linear equilibrium structure. The geometry of the $\text{C}_2\text{H}-\text{H}_2$ system was described by four internal Jacobi coordinates. The z -axis of the body-fixed frame is aligned with the intermolecular vector \mathbf{R} connecting the centre of masses of the two molecules. The orientation of C_2H and H_2 relative to \mathbf{R} is defined by the polar angles θ and θ' , respectively, while the dihedral angle φ characterizes the angle between the two half-planes containing the C_2H and H_2 molecules.

In Paper I, only the collisional excitation of C_2H by *para*- H_2 was considered. Indeed, for collisions at a low temperature, the probability of rotational excitation of H_2 is low so that the collision is well described using an interaction potential obtained by an average over angular motion of the H_2 molecule (Lique et al. 2008). Thus, the *ab initio* calculations were performed on

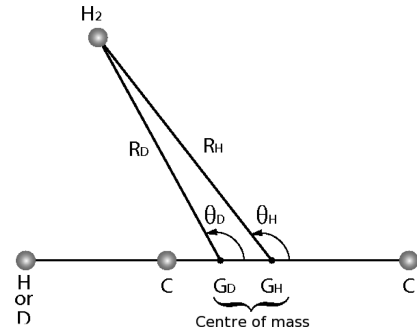


Figure 1. Jacobi coordinates for $\text{C}_2\text{H}-\text{H}_2$ - and $\text{C}_2\text{D}-\text{H}_2$ -averaged potential energy surfaces.

a two-dimensional (2D) grid of (R, θ) coordinates for three selected orientations of the H_2 molecule, defined by (θ', φ) angles with fixed values $(\pi/2, 0)$, $(\pi/2, \pi/2)$ and $(0, 0)$ and the $\text{C}_2\text{H}-\text{H}_2$ -averaged PES was obtained at each set of (R, θ) by an equipoise averaging over these three selected orientations. The aug-cc-pVTZ basis set of Woon & Dunning (1994) was used for the five atoms, together with the $[3s3p2d1f]$ bond functions of Williams et al. (1995) which were placed at the mid-distance between the C_2H and H_2 centres of masses. Calculations of the PES were performed with the partially spin-restricted coupled-cluster calculations at the RCCSD(T) level of theory (Knowles, Hampel & Werner 1993) with frozen core orbitals. The resulting energies have been corrected for the basis set superposition error using the Boys & Bernardi (1970) counterpoise procedure. All *ab initio* calculations have been carried out with the MOLPRO suite of programs (Werner et al. 2012).

The 2D grid included 30 values of the intermolecular distance R ranging from 4.8 to $25a_0$, with the angle θ varying uniformly from 0° to 180° by steps of 10° .

The calculated $V_{\text{av}}(R, \theta)$ interaction energies averaged over H_2 rotation were finally fitted to the form of equation (1) following the procedure described by Werner et al. (1989), including expansion functions P_l up to $l_{\text{max}} = 36$ to represent the overall anisotropy:

$$V_{\text{av}}(R, \theta) = \sum_l V_l(R) P_l(\cos \theta), \quad (1)$$

The global minimum was found for the linear C-C-H-H arrangement at $R = 8.23a_0$ and $\theta = 180^\circ$, with an associated well depth of -61.03 cm^{-1} relative to the $\text{C}_2\text{H}-\text{H}_2$ dissociation limit. A secondary minimum of -58.29 cm^{-1} is found at $R = 7.35a_0$ and $\theta = 39^\circ$.

Within the Born–Oppenheimer approximation, the electronic ground state potential is the same for $\text{C}_2\text{H}-\text{H}_2$ and $\text{C}_2\text{D}-\text{H}_2$ and only depends on the mutual distances of the atoms. As $\text{C}_2\text{H}-\text{H}_2$ was calculated at the C_2H equilibrium distance (i.e. we neglect the zero-point energy correction), we could use the same intermolecular distance for the $\text{C}_2\text{D}-\text{H}_2$ PES. The only difference between the two PESs is the position of the centre of mass taken for the origin of the Jacobi coordinates (see Fig. 1). For $\text{C}_2\text{D}-\text{H}_2$, we have taken into account the effect of the displacement of the centre of mass and hence used new Jacobi coordinates R_D and θ_D instead of R_H and θ_H (Dumouchel et al. 2012).

The centre-of-mass displacement leads to a different expansion (equation 1) of the $\text{C}_2\text{D}-\text{H}_2$ PES over the Legendre polynomials compared to the $\text{C}_2\text{H}-\text{H}_2$ PES. The dependence on R of the two expansions is displayed in Fig. 2.

First, we note that the differences are very small except for the $\lambda = 1$ coefficient that is smaller in the case of $\text{C}_2\text{D}-\text{H}_2$ than

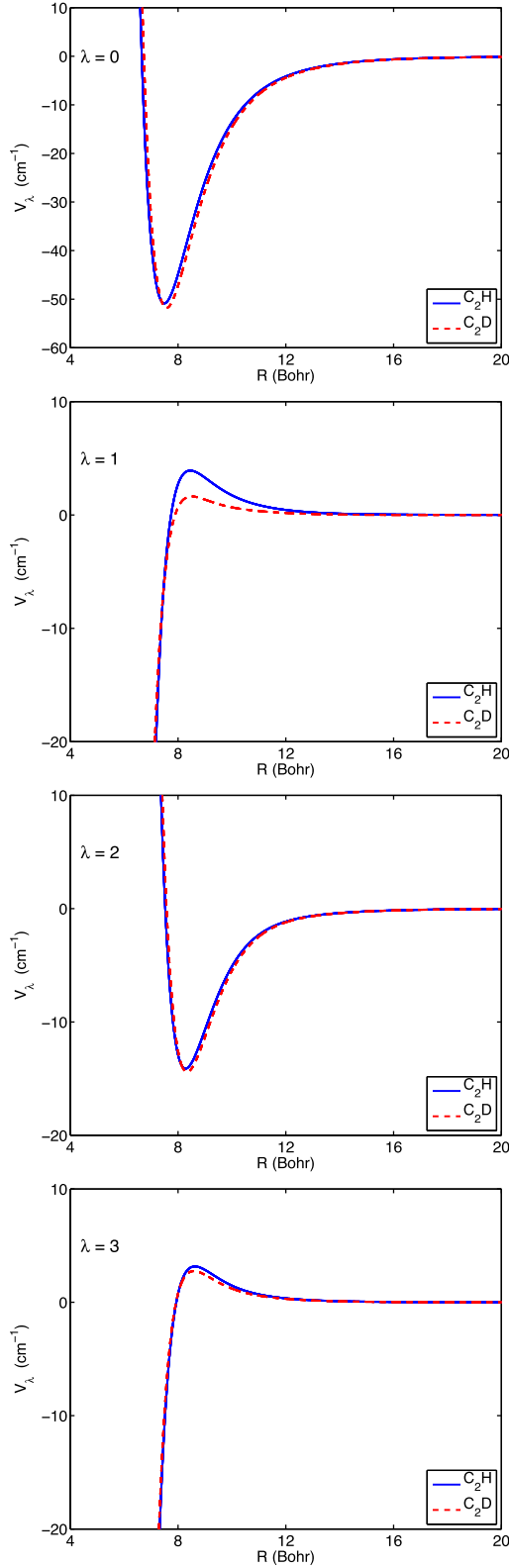


Figure 2. Plot of the first four radial Legendre expansion coefficients ($\lambda = 0, \dots, 3$) as a function of R . Solid lines denote C_2H-H_2 while dashed lines denote C_2D-H_2 .

Table 1. Fine-structure energies of the C_2H and C_2D molecules.

N	j	E (cm^{-1}) C_2H	E (cm^{-1}) C_2D
0	0.5	0.000	0.000
1	1.5	2.913	2.405
1	0.5	2.916	2.408
2	2.5	8.739	7.217
2	1.5	8.744	7.221
3	3.5	17.478	14.434
3	2.5	17.486	14.441
4	4.5	29.131	24.057
4	3.5	29.140	24.066
5	5.5	43.696	36.086
5	4.5	43.708	36.097
6	6.5	61.174	50.521
6	5.5	61.188	50.533
7	7.5	81.564	67.360
7	6.5	81.579	67.374
8	8.5	104.864	86.604
8	7.5	104.882	86.620

in the case of C_2H-H_2 . This reflects a smaller anisotropy of the C_2D-H_2 PES that could influence the values of the corresponding rate coefficients.

2.2 Scattering calculations

The main focus of this work is to determine hyperfine-resolved integral cross-sections and rate coefficients of C_2H and C_2D in collision with $H_2(j=0)$. As the rotational structure of H_2 is neglected, the problem, in terms of scattering calculations, is equivalent to the collisional excitation of the rigid rotor C_2H and C_2D by a structureless atom.

The rotational levels of C_2H and C_2D were computed from experimental spectroscopic constants of Killian, Gottlieb & Thaddeus (2007). The energies of the first 17 fine-structure levels of C_2H and C_2D considered in this work are given in Table 1. As can be seen in Table 1, the rotational structures of the two species are different. Due to the smaller rotational constants of C_2D , the energy differences between the C_2D levels are smaller than for the C_2H levels.

The hyperfine splitting of the C_2H and C_2D levels is very small (about 0.002 cm^{-1}). Hence, as the hyperfine levels can be assumed to be degenerate (i.e. same energy as that of the associated fine structure level), it is possible to considerably simplify the hyperfine scattering problem.

The integral cross-sections corresponding to transitions between hyperfine levels of the C_2H and C_2D molecules can be obtained from the scattering nuclear spin-free S -matrix using a recoupling method (Alexander & Dagdigan 1985; Faure & Lique 2012). Within such approach, we first perform nuclear spin-free close-coupling calculations to obtain the $S'(Nj|N'j')$ diffusion matrix elements between C_2H (C_2D) fine-structure levels, where J denotes the total angular momentum (without including the nuclear spin of the target) and l the relative orbital angular momentum ($\mathbf{J} = \mathbf{j} + \mathbf{l}$). Then, the total angular momentum J_T of the colliding system including the nuclear spin is given by

$$\mathbf{J}_T = \mathbf{J} + \mathbf{I}.$$

In the recoupling scheme, inelastic cross-sections associated with a transition from an initial hyperfine level NjF to a final hyperfine

level $N'j'F'$ were thus obtained as follows:

$$\sigma_{NjF \rightarrow N'j'F'} = \frac{\pi}{k_{NjF}^2} \frac{1}{2F+1} \sum_{J_T} (2J_T+1) \times \sum_{I'} |\delta_{NN'} \delta_{jj'} \delta_{II'} \delta_{FF'} - S^{J_T}(NjIF|N'j'I'F')|^2, \quad (2)$$

where $S^{J_T}(NjIF|N'j'I'F')$ denotes the S -matrix for that total angular momentum J_T associated with a transition from an initial hyperfine level NjF to a final hyperfine level $N'j'F'$. The transformation between the S^{J_T} -matrix elements and the nuclear spin-free S^J -matrix is given by

$$S^{J_T}(NjIF|N'j'I'F') = \sum_J [(2F+1)(2F'+1)]^{1/2} (2J+1) \times (-1)^{F+F'+I+I'-2J} \begin{Bmatrix} I & j & J \\ I & J_T & F \end{Bmatrix} \times \begin{Bmatrix} I' & j' & J \\ I & J_T & F' \end{Bmatrix} S^J(NjI|N'j'I'). \quad (3)$$

From the rotationally inelastic cross-sections $\sigma_{NjF \rightarrow N'j'F'}(E_c)$, one can obtain the corresponding thermal rate coefficients at temperature T by an average over the collision energy (E_c):

$$k_{NjF \rightarrow N'j'F'}(T) = \left(\frac{8}{\pi \mu (k_B T)^3} \right)^{1/2} \times \int_0^\infty \sigma_{NjF \rightarrow N'j'F'}(E_c) E_c e^{-\frac{E_c}{k_B T}} dE_c, \quad (4)$$

where k_B is the Boltzmann's constant and the integral extends over all values of the collision energy.

Recent scattering calculations considering the fine structure excitation of C_2H by *para*- H_2 ($j=0$) have been published in Paper I. We use the same methodology to calculate the fine-structure-resolved scattering matrices, cross-sections and rate coefficients for C_2D . Hyperfine-resolved C_2H and C_2D cross-sections and rate coefficients are obtained from fine-structure-resolved scattering matrices using the transformation given by equation (3). The reduced mass of the C_2H-H_2 system is $\mu = 1.8655$ amu whereas the reduced mass of C_2D-H_2 is $\mu = 1.8707$ amu. All the scattering calculations were performed with the HIBRIDON scattering program.¹

3 RESULTS

3.1 Hyperfine structure excitation

Figs 3 and 4 present the temperature variation of the hyperfine C_2H-H_2 and C_2D-H_2 rate coefficients, respectively, for the selected $\Delta j = \Delta N$ and $\Delta j \neq \Delta N$ transitions.

From these figures, one can see a propensity for $\Delta j = \Delta N$ transitions whatever the hyperfine states F are. A strong propensity in the favour of $\Delta F = \Delta j$ transitions is also observed confirming that hyperfine rate coefficients cannot be accurately estimated from fine-structure rate coefficients using approximate formulae, such as the

¹ The HIBRIDON package was written by M. H. Alexander, D. E. Manolopoulos, H.-J. Werner and B. Follmeg, with contributions by P. F. Vohralik, D. Lemoine, G. Corey, R. Gordon, B. Johnson, T. Orlikowski, A. Berning, A. Degli-Esposti, C. Rist, P. Dagdigian, B. Pouilly, G. van der Sanden, M. Yang, F. de Weerd, S. Gregurick, J. Klos and F. Lique. <http://www2.chem.umd.edu/groups/alexander/>

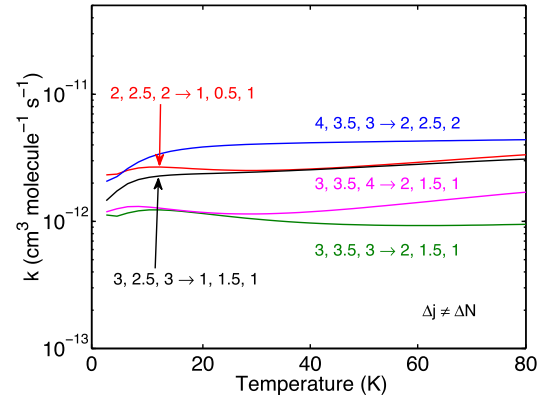
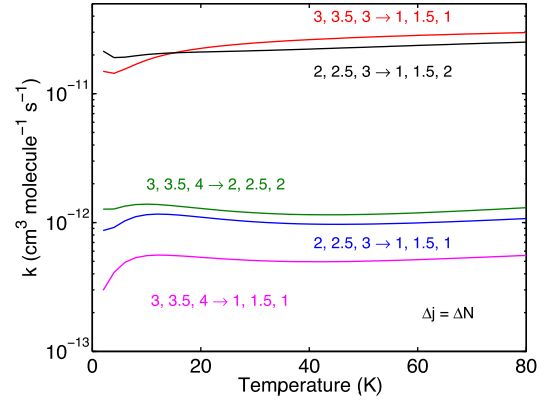


Figure 3. Temperature dependence of variation of the hyperfine-resolved C_2H-H_2 rate coefficients for the selected $\Delta j = \Delta N$ and $\Delta j \neq \Delta N$ transitions.

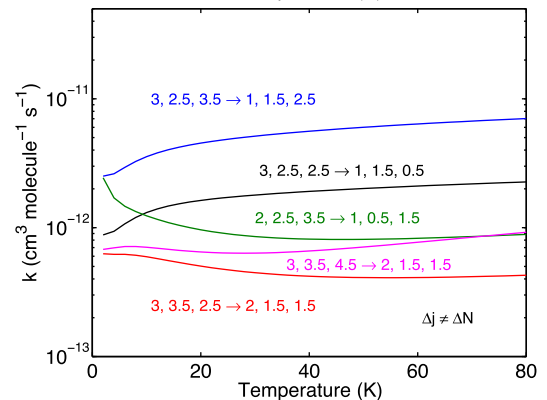
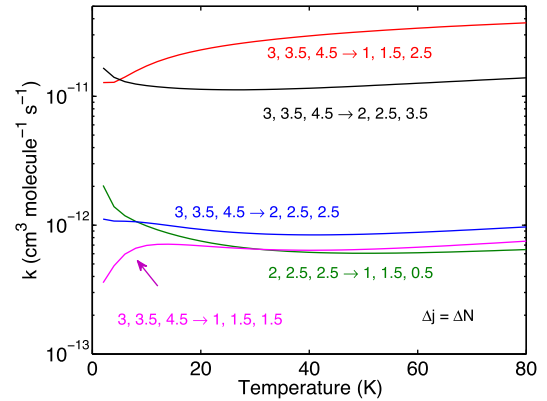


Figure 4. Temperature dependence of variation of the hyperfine-resolved C_2D-H_2 rate coefficients for the selected $\Delta j = \Delta N$ and $\Delta j \neq \Delta N$ transitions.

M_j randomizing limit. The same trends, predicted theoretically by Alexander & Dagdigan (1985), were obtained recently for CN–He (Lique & Klos 2011), CN– H_2 (Kalugina, Lique & Klos 2012), C_2H –He (Spielfiedel et al. 2013) and NH/ND–He (Dumouchel et al. 2012) collisions.

The complete set of (de-)excitation rate coefficients will be made available through the LAMDA (Schöier et al. 2005) and BASECOL (Dubernet et al. 2013) data bases.

3.2 Comparison between C_2H – H_2 and C_2D – H_2 rate coefficients

It is generally assumed that collisional rate coefficients of the main isotopologue can be used to estimate rate coefficients for the secondary isotopologues. This approximation is reliable in the case of heavy atom substitution, as found for ^{13}C versus ^{12}C (Flower & Lique 2015) and ^{15}N versus ^{14}N (Daniel et al. 2016), but is questionable in the case of H/D substitution, as observed in the case of H_2O/D_2O (Scribano, Faure & Wiesenfeld 2010), NH/ND (Dumouchel et al. 2012) and to a lesser extent for HCO^+/DCO^+ (Buffa, Dore & Meuwly 2009; Buffa 2012).

C_2H and C_2D molecules do not have the same hyperfine structure. So hereafter we compare their respective fine-structure-resolved rate coefficients (i.e. rate coefficients summed over the final hyperfine structure). This comparison is performed between de-excitation rate coefficients to avoid the existing threshold effects when excitation rate coefficients are considered.

Fig. 5 presents the thermal dependence of the state-to-state C_2H and C_2D rate coefficients for a selection of $\Delta j = \Delta N = 1$, $\Delta j = \Delta N = 2$ and $\Delta j \neq \Delta N$ transitions. One can clearly see that the C_2H and C_2D rate coefficients are different, especially for transitions with $\Delta j = \Delta N = 1$ that correspond to the radiative transitions.

We report in Fig. 6 the C_2D – H_2 de-excitation rate coefficients at 30 K as a function of the C_2H – H_2 ones, for all fine-structure-resolved transitions $N, j \rightarrow N', j'$ with $N, N' \leq 8$. All the rate coefficients agree within a factor two. The dominant C_2H – H_2 and C_2D – H_2 rate coefficients corresponding to $\Delta j = \Delta N = 2$ transitions are in very good agreement. On the contrary, C_2D – H_2 data for $\Delta j = \Delta N = 1$ transitions are systematically lower than the C_2H – H_2 data.

As discussed in Dumouchel et al. (2012), three effects may explain the differences due to D/H substitution:

- (i) The reduced masses of C_2H – H_2 (1.8655 amu) and C_2D – H_2 (1.8707 amu) differ.
- (ii) The rotational constants of C_2H and C_2D are not the same.
- (iii) The different positions of the centre of mass (see Fig. 1) modify the PES expansion.

Considering the small differences in the reduced masses of the two species, one can estimate that the difference obtained in the $\Delta j = \Delta N = 1$ rate coefficients could come from the effects (ii) and (iii). Most probably, the difference is induced by effect (iii) as effect (ii) would affect the data for all the transitions. The difference in the position of the centre of mass leads to a different C_2D – H_2 and C_2H – H_2 PESs expansion and thus different the magnitude of cross-sections and rate coefficients. Indeed, Fig. 2 shows that the V_1 radial coefficient is larger for C_2H than for C_2D . As this term directly couples two levels with $\Delta j = \Delta N = 1$, it is not surprising that, for $\Delta j = \Delta N = 1$ transitions, the C_2H – H_2 rate coefficients are larger than those of C_2D – H_2 .

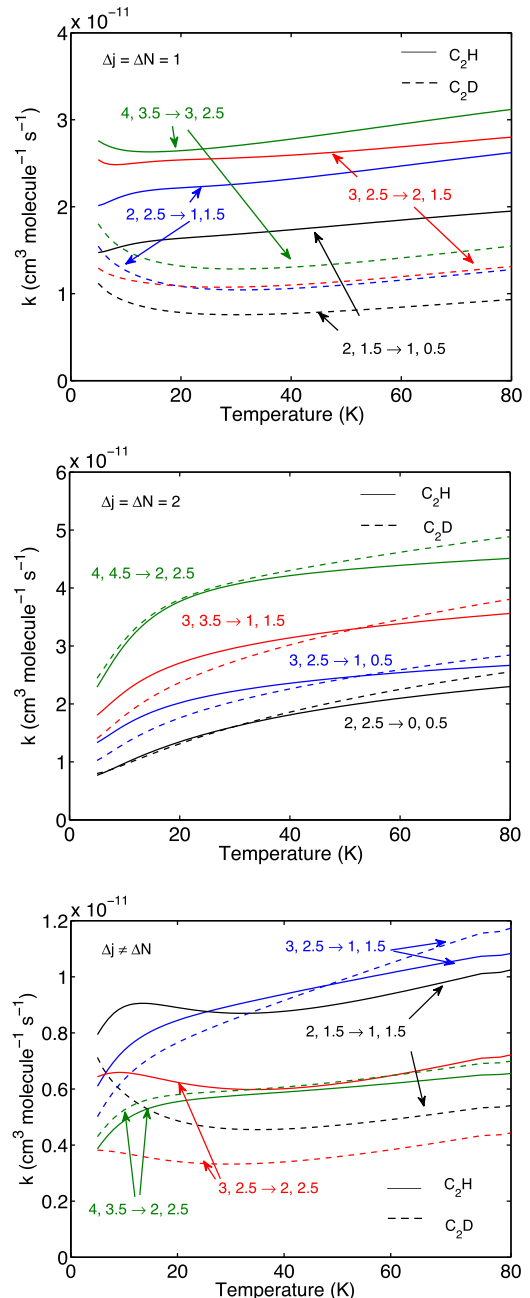


Figure 5. Temperature variation of the fine-structure-resolved C_2H – H_2 (solid line) and C_2D – H_2 (dashed line) de-excitation rate coefficients for the selected $N, j \rightarrow N', j'$ transitions.

4 SUMMARY AND CONCLUSION

The hyperfine excitation of both C_2H and C_2D have been investigated. We have obtained rate coefficients for the lowest levels and temperatures ranging from 5 to 80 K. As found previously for the excitation of C_2H by He and for many other systems, the $\Delta N = \Delta j = \Delta F$ propensity rule is observed for the hyperfine transitions for both isotopologues.

The comparison between C_2H and C_2D rate coefficients shows that the two sets of data differ by less than a factor two on average, the largest difference being obtained for $\Delta j = \Delta N = 1$ transitions. This difference is explained by the different positions of the centre of masses of the two species in interaction with H_2 . Such a difference

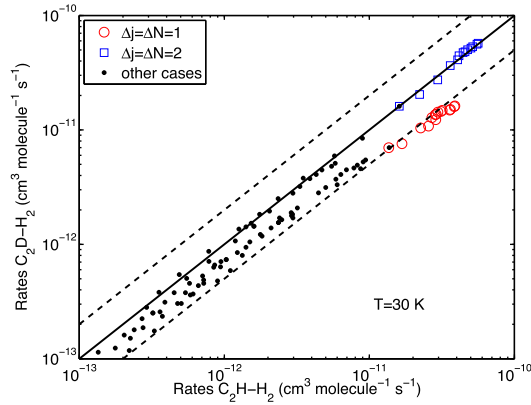


Figure 6. Comparison between C_2H-H_2 and C_2D-H_2 rate coefficients at 30 K. Blue squares denote rates for $\Delta j = \Delta N = 2$ transitions, red circles denote rates for $\Delta j = \Delta N = 1$ transitions and black markers denote rates for all other transitions. The straight lines show equal C_2H-C_2D rates (full line) and C_2H rates multiplied and divided by 2 (dashed lines).

could be crucial for the astrophysical modelling since these rate coefficients correspond to the radiative transitions that are usually detected.

Indeed, the magnitude of the emission lines is proportional to the population of the excited states of the molecules in the interstellar clouds. Two processes contribute to the population of the excited states, and the radiative and the collisional processes. The magnitude of the emission lines will hence depend on the magnitude of both the dipole moment and the collisional rate coefficients. As C_2H and C_2D molecules share the same dipole moment, the intensity of the emission lines will mainly depend on the magnitude of the rate coefficients.² In this study, we found that the C_2H rate coefficients for transitions with $|\Delta j| = 1$ are stronger by a factor $\simeq 2$ than that of C_2D . Hence, C_2H should then present a stronger emission spectrum than C_2D , assuming that the two molecules are present in the same environment and under similar physical conditions. Such results should lead to a decrease in the $[C_2H]/[C_2D]$ abundance ratio derived in previous studies (Combes et al. 1985; Vrtilik et al. 1985) as none of these studies consider the different excitation mechanism of the two isotopologues. More generally, the present calculations imply that an accurate determination of the $[C_2H]/[C_2D]$ abundance ratio will rely on non-LTE analysis using both collisional and radiative data.

ACKNOWLEDGEMENTS

The authors acknowledge their friend and colleague Annie Spielfiedel who actively participated in the work that leads to this paper. Annie Spielfiedel passed away on 2016 December 14. We dedicate this paper to her memory.

This work was supported by the CNRS program ‘Physique et Chimie du Milieu Interstellaire’ (PCMI) co-funded by the Centre National d’Etudes Spatiales (CNES).

² The different rotational constants can also influence the magnitude of the emission lines since the radiative Einstein coefficients will be different. However, we expect that such effect will be moderate, especially when analysing the emission spectra from the first rotational states.

This research was also supported by the French National Research Agency (ANR) through a grant to the Anion Cos Chem project (ANR-14-CE33-0013).

Part of the calculations were performed using HPC resources from GENCI-[CINES/IDRIS] (grant no. 2010040883) and on work stations at the Centre Informatique of Paris Observatory.

REFERENCES

- Alexander M. H., Dagdigan P. J., 1985, *J. Chem. Phys.*, 83, 2191
 Beuther H., Semenov D., Henning T., Linz H., 2008, *ApJ*, 675, L33
 Boys S. F., Bernardi F., 1970, *Mol. Phys.*, 19, 553
 Brünken S., Gottlieb C. A., Gupta H., McCarthy M. C., Thaddeus P., 2007, *A&A*, 464, L33
 Buffa G., 2012, *MNRAS*, 421, 719
 Buffa G., Dore L., Meuwly M., 2009, *MNRAS*, 397, 1909
 Combes F., Boulanger F., Encrenaz P. J., Gerin M., Bogey M., Demuyneck C., Destomb J. L., 1985, *A&A*, 147, L25
 Cuadrado S., Goicoechea J. R., Pilleri P., Cernicharo J., Fuente A., Joblin C., 2015, *A&A*, 575, A82
 Daniel F. et al., 2016, *A&A*, 592, A45
 Dubernet M.-L. et al., 2013, *A&A*, 553, A50
 Dumouchel F., Klos J., Toboła R., Bacmann A., Maret S., Hily-Blant P., Faure A., Lique F., 2012, *J. Chem. Phys.*, 137, 114306
 Dutrey A., Guilloteau S., Guélin M., 1997, *A&A*, 317, L55
 Faure A., Lique F., 2012, *MNRAS*, 425, 740
 Faure A., Wiesenfeld L., Scribano Y., Ceccarelli C., 2012, *MNRAS*, 420, 699
 Flower D. R., Lique F., 2015, *MNRAS*, 446, 1750
 Gottlieb C. A., Gottlieb E. W., Thaddeus P., 1983, *ApJ*, 264, 740
 Guélin M., Langer W. D., Wilson R. W., 1982, *A&A*, 107, 107
 Guilloteau S., Piétu V., Dutrey A., Guélin M., 2006, *A&A*, 448, L5
 Hatchell J., Millar T. J., Rodgers S. D., 1998, *A&A*, 332, 695
 Kalugina Y., Lique F., Klos J., 2012, *MNRAS*, 422, 812
 Killian T. C., Gottlieb C. A., Thaddeus P., 2007, *J. Chem. Phys.*, 127, 114320
 Knowles P. J., Hampel C., Werner H.-J., 1993, *J. Chem. Phys.*, 99, 5219
 Leurini S. et al., 2006, *A&A*, 454, L47
 Lique F., Klos J., 2011, *MNRAS*, 413, L20
 Lique F., Toboła R., Klos J., Feautrier N., Spielfiedel A., Vincent L. F. M., Chafasiński G., Alexander M. H., 2008, *A&A*, 478, 567
 Lucas R., Liszt H. S., 2000, *A&A*, 358, 1069
 Müller H. S. P., Klaus T., Winnewisser G., 2000, *A&A*, 357, L65
 Najaf F., Ben Abdallah D., Spielfiedel A., Dayou F., Lique F., Feautrier N., 2014, *Chem. Phys. Lett.*, 614, 251
 Padovani M., Walmsley C. M., Tafalla M., Galli D., Müller H. S. P., 2009, *A&A*, 505, 1199
 Pety J., Teyssier D., Fossé D., Gerin M., Roueff E., Abergel A., Habart E., Cernicharo J., 2005, *A&A*, 435, 885
 Roberts H., Millar T. J., 2000, *A&A*, 361, 388
 Saleck A. H., Simon R., Winnewisser G., Wouterloot J., 1994, *Can. J. Phys.*, 72, 747
 Sastry K. V. L. N., Helminger P., Charo A., Herbst E., De Lucia F. C., 1981, *ApJ*, 251, L119
 Schöier F. L., van der Tak F. F. S., van Dishoeck E. F., Black J. H., 2005, *A&A*, 432, 369
 Scribano Y., Faure A., Wiesenfeld L., 2010, *J. Chem. Phys.*, 133, 231105
 Spielfiedel A., Feautrier N., Najaf F., Ben D. A., Dayou F., Senent M. L., Lique F., 2013, *MNRAS*, 429, 923
 Teyssier D., Fossé D., Gerin M., Pety J., Abergel A., Roueff E., 2004, *A&A*, 417, 135
 Treviño-Morales S. P. et al., 2014, *A&A*, 569, A19
 Tucker K. D., Kutner M. L., Thaddeus P., 1974, *ApJ*, 193, L115
 van Dishoeck E. F., Thi W.-F., van Zadelhoff G.-J., 2003, *Astrophys. Space Sci.*, 285, 691

Vrtilek J. M., Gottlieb C. A., Langer W. D., Thaddeus P., Wilson R. W., 1985, *ApJ*, 296, L35
Werner H.-J., Follmeg B., Alexander M. H., Lemoine D., 1989, *J. Chem. Phys.*, 91, 5425
Werner H.-J., Knowles P. J., Knizia G., Manby F. R., Schütz M., 2012, *WIREs Comput. Mol. Sci.*, 2, 242
Wiesenfeld L., Scribano Y., Faure A., 2011, *Phys. Chem. Chem. Phys.*, 13, 8230

Williams H. L., Mas E. M., Szalewicz K., Jeziorski B., 1995, *J. Chem. Phys.*, 103, 7374
Woon D. E., Dunning Jr T. H., 1994, *J. Chem. Phys.*, 100, 2975

This paper has been typeset from a $\text{\TeX}/\text{\LaTeX}$ file prepared by the author.